Figures and figure supplements

DPP9 is a novel component of the N-end rule pathway targeting the tyrosine kinase Syk

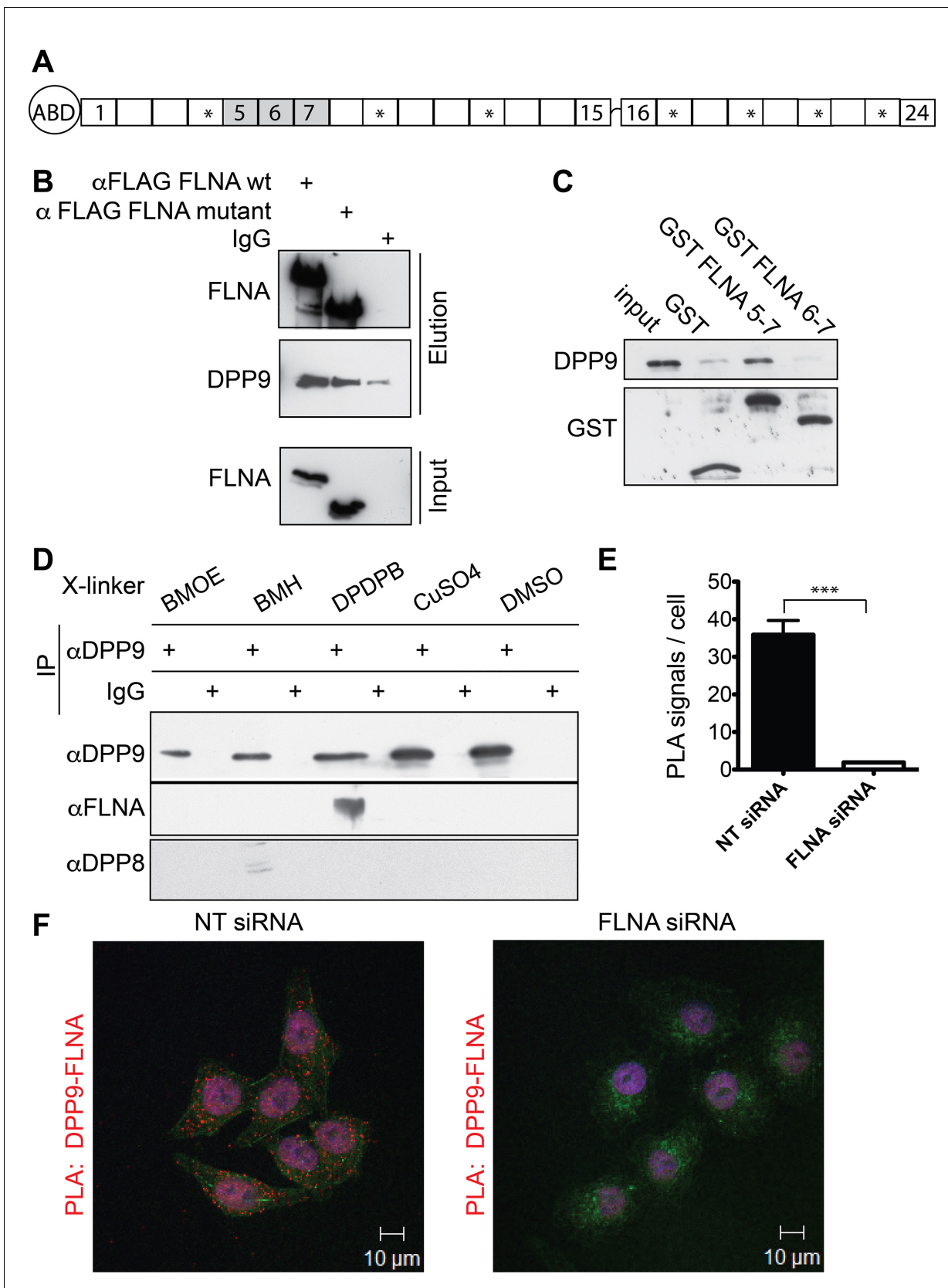**Daniela Justa-Schuch** *et al*

Figure 1. Filamin A (FLNA) is a novel DPP9 interacting protein. (A) Schematic representation of FLNA structure including numbering of the Ig-like domain repeats, and labelling of the actin-binding domain (ABD). The asterisks mark the repeats lacking in the FLNA variant form used in (B). (B) Pull-

Figure 1 continued on next page

Figure 1 continued

down assays showing direct interaction between recombinant DPP9 and recombinant FLAG tagged wt FLNA or a mutated form of FLAG-FLNA (lacking repeats 4, 9, 12, 17, 19, 21, and 23). Shown is a representative result of at least three independent experiments. (C) Recombinant DPP9 binds directly to GST- FLNA construct containing repeats 5–7 but not to GST-FLNA construct containing repeats 6–7. Shown is a representative result of at least three independent experiments. (D) Co-immunoprecipitation of endogenous FLNA with endogenous DPP9 from HeLa cells treated with different cross-linkers. Binding was observed in the presence of the sulfhydryl cross-linker DPDPB. Shown is a representative result of at least three independent experiments. To control for the specificity of the cross link, we blotted for DPP8, which did not bind to DPP9 in the presence of DPDPB (E) Quantification of the proximity ligation assay (in situ PLA) visualizing DPP9-FLNA interaction in HeLa cells treated with FLNA silencing oligos or non-targeting (NT) siRNAs for control shown in (F). The number of PLA signals per cell were quantified in a blinded manner using the Duolink ImageTool software (SIGMA). Data are represented as mean ± SEM. Signals of more than 130 cells were quantified for each condition respectively. Statistical analysis was carried out by an unpaired two-tailed t test (***p<0.0005). (F) PLA showing interaction of DPP9 with FLNA in HeLa cells. Each red dot represents a single FLNA-DPP9 interaction. The number of PLA signals is significantly decreased in cells silenced for FLNA compared to cells treated with NT siRNA. Actin filaments are stained in green, nuclei were visualized by using HOECHST. Shown are representative images of at least three independent PLA experiments.
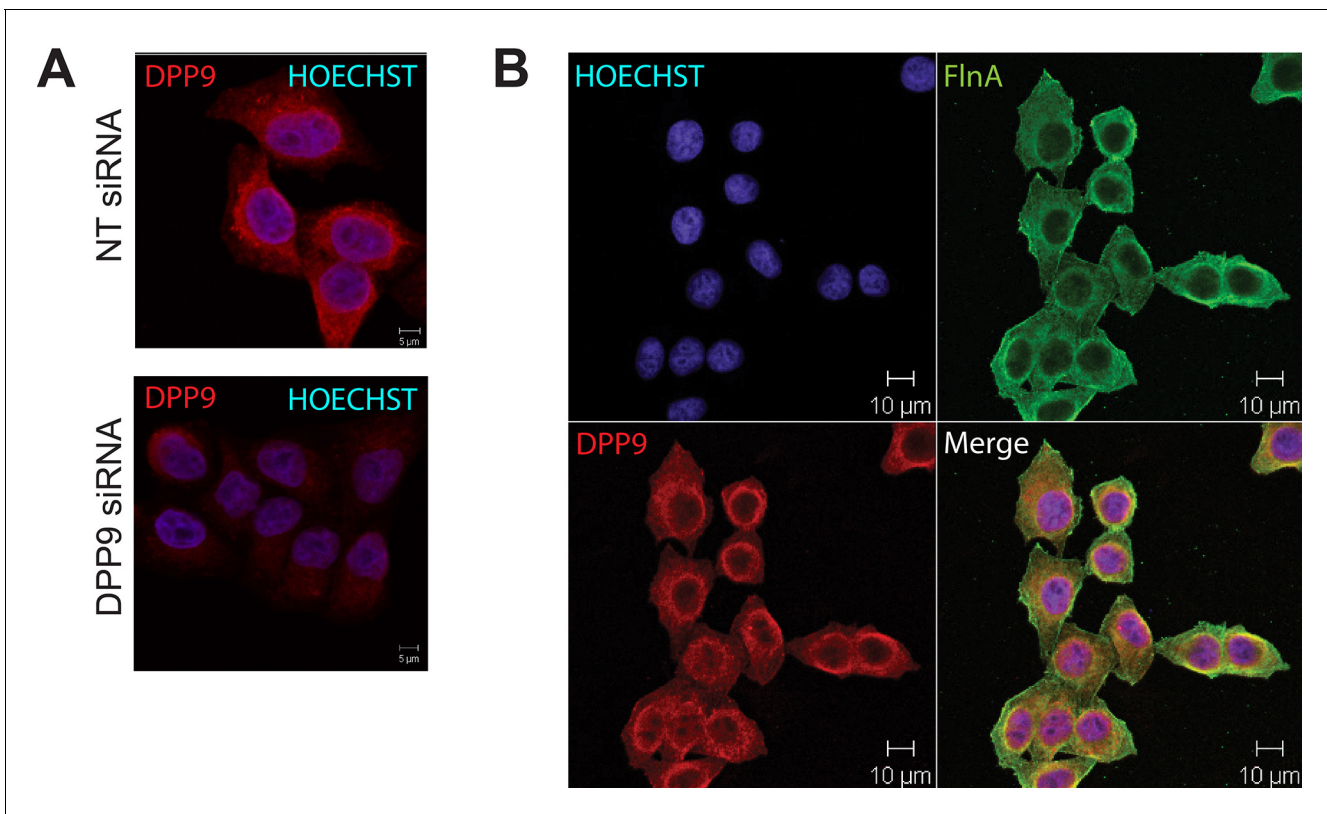
Figure 1—figure supplement 1. Co localization of DPP9 and FLNA. (**A**) Immunofluorescence microscopy images of HeLa cells decorated with goat anti-DPP9 antibody. To test for the specificity of the antibody, cells were treated with DPP9 targeting siRNA, control cells were treated with non-targeting (NT) siRNA oligonucleotides. Nuclei were stained with HOECHST. Indirect immunofluorescence images show that DPP9 signals are clearly reduced in DPP9-silenced cells. These experiments were repeated at least three times. (**B**) Immunofluorescence images showing an overlap in the localization of FLNA and DPP9. HeLa cells were decorated with goat anti-DPP9 and a commercial anti-FLNA antibody. Nuclei were visualized by HOECHST staining. These experiments were repeated at least three times.
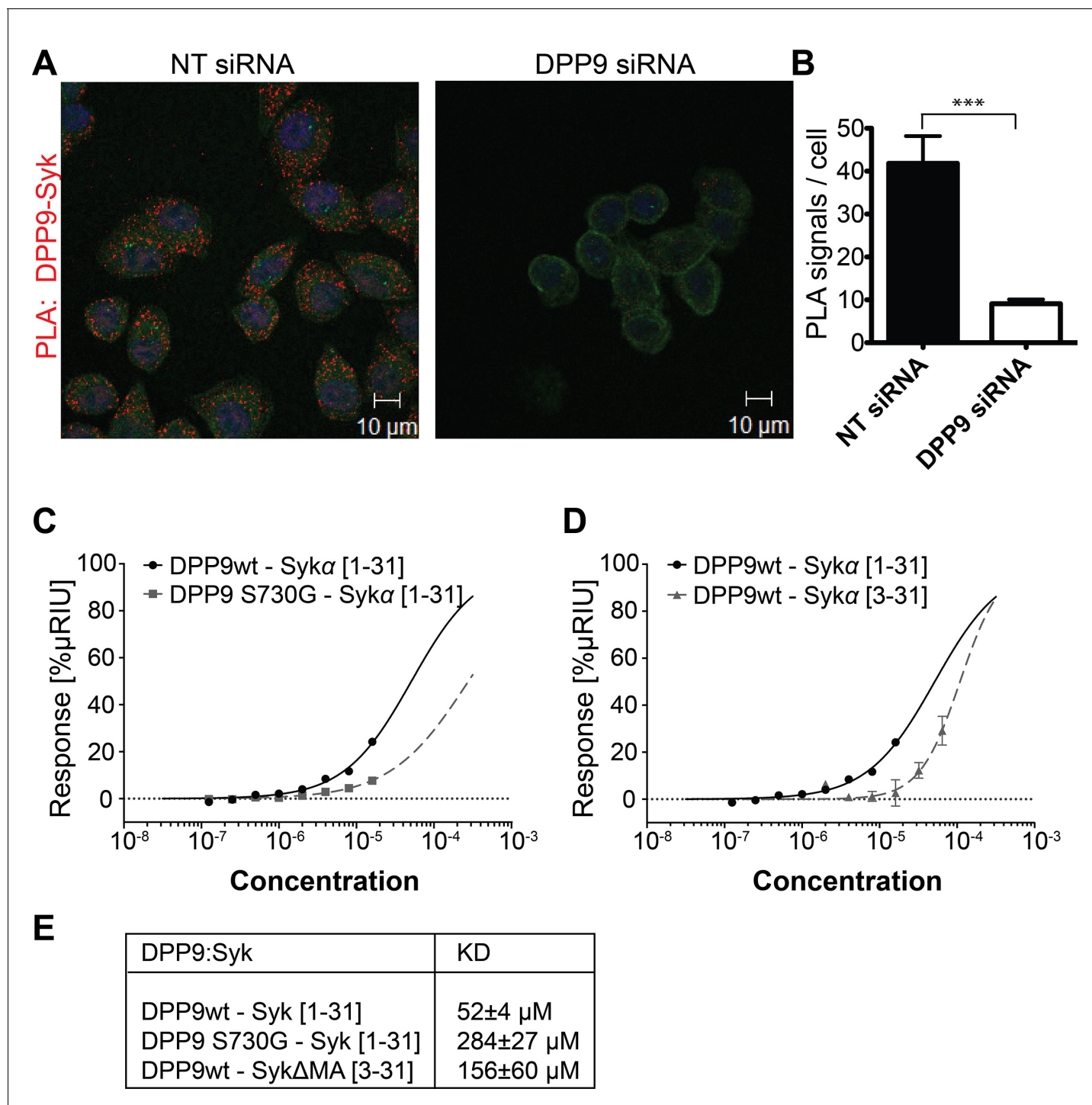DOI: 10.7554/eLife.16370.004

Figure 2. DPP9 interacts with the amino terminus of the tyrosine kinase Syk. (**A**) PLA in HeLa cells showing interaction of DPP9 with Syk. The number of PLA signals (red) representing DPP9-Syk interaction is significantly reduced in cells silenced for DPP9 compared to cells treated with NT siRNAs. Shown are representative images of at least three independent PLA experiments. Actin filaments are stained in green, nuclei are visualized with HOECHST staining. (**B**) Quantification of the PLA DPP9-Syk shown in (**A**). Data are represented as mean ± SEM. Signals of more than 150 cells for each condition were quantified respectively in a blinded manner using the Duolink ImageTool software (SIGMA). Statistical analysis was carried out by an unpaired two-tailed t test (***$p < 0.0005$). (**C**) Surface Plasmon Resonance (SPR) assays showing direct interaction between DPP9 wild type and a synthetic peptide covering the first 31 amino acids of Syk (1–31). The binding affinity of the Syk (1–31) peptide is lower towards the inactive DPP9 variant (DPP9 S730G). Depicted are equilibrium binding isotherms obtained from at least three repetitions for respective interaction pairs of recombinant DPP9 and DPP9 S730G with Syk (1–31) peptides. DPP9 was immobilized at the chip surface and the Syk (1–31) peptide was injected over the surface with concentrations

Figure 2 continued on next page

Figure 2 continued

varying from 16 µM to 0.125 µM. Binding affinities were calculated using Graph Pad Prism 6.0. The Error is displayed as SEM. (**D**) Surface Plasmon Resonance (SPR) assays showing that the interaction of DPP9 with the peptide corresponding to Syk N-terminus requires the first two residues in Syk N-terminus. Depicted are equilibrium binding isotherms obtained from at least three repetitions for respective interaction pairs of recombinant DPP9 with Syk (1–31) or Syk (3–31) peptides. Recombinant His-tagged DPP9 was immobilized on the chip surface and the Syk (1–31) or Syk (3–31) peptide was injected over the surface with concentrations varying from 16 µM to 0.125 µM for Syk (1–31) and 32 µM to 1 µM for Syk (3–31). Binding affinities were calculated as described in (**C**). (**E**) Table summarizing the K_D values.
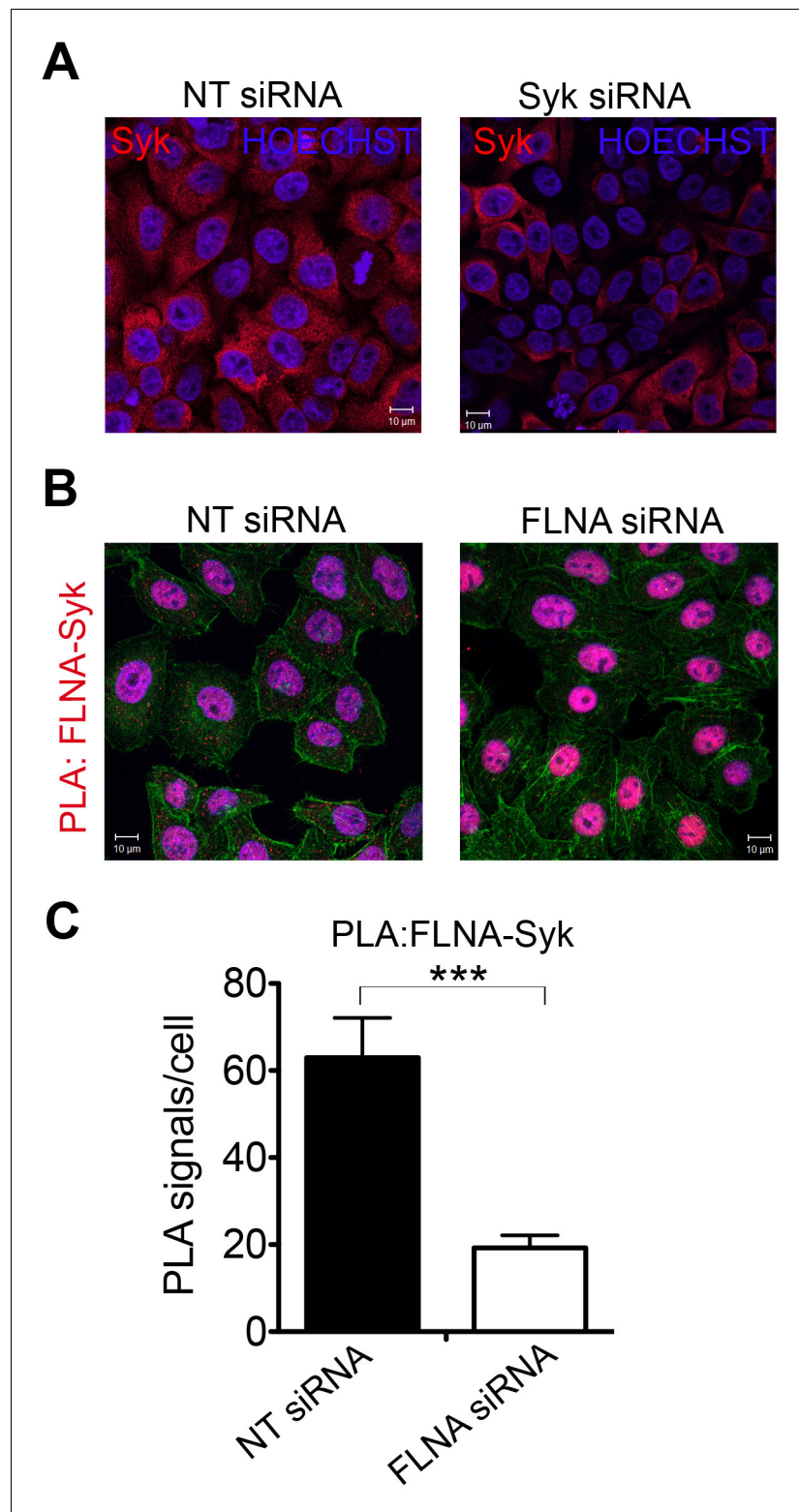
DOI: 10.7554/eLife.16370.005

Figure 2—figure supplement 1. Interaction of FLNA with Syk is conserved in HeLa cells. (**A**) Syk is expressed in HeLa cells as shown by indirect immunofluorescence using a Syk-specific antibody. To test for specificity of the antibody cells were treated with Syk targeting siRNA, control cells were treated with non-targeting (NT) siRNA oligonucleotides. Syk signals were clearly decreased in Syk-silenced cells. HOECHST staining was applied to stain nuclei. (**B**) Interaction of Syk with FLNA in HeLa cells shown by PLA using FLNA- and Syk-specific antibodies. The

Figure 2—figure supplement 1 continued on next page

Figure 2—figure supplement 1 continued

number of PLA signals was markedly decreased in cells treated with siRNA against FLNA compared to control cells treated with non-targeting (NT) siRNA. Actin filaments are stained in green, nuclei were visualized by using HOECHST. Shown are representative images of at least three independent PLA experiments. (**C**) Quantification of the PLA FLNA-Syk in HeLa cells shown in (**B**). Data are represented as mean ± SEM. Signals of more than 150 cells for each condition were quantified in a blinded manner using the Duolink ImageTool (SIGMA). Statistical analysis was carried out by an unpaired two-tailed t test (***p<0.0005).
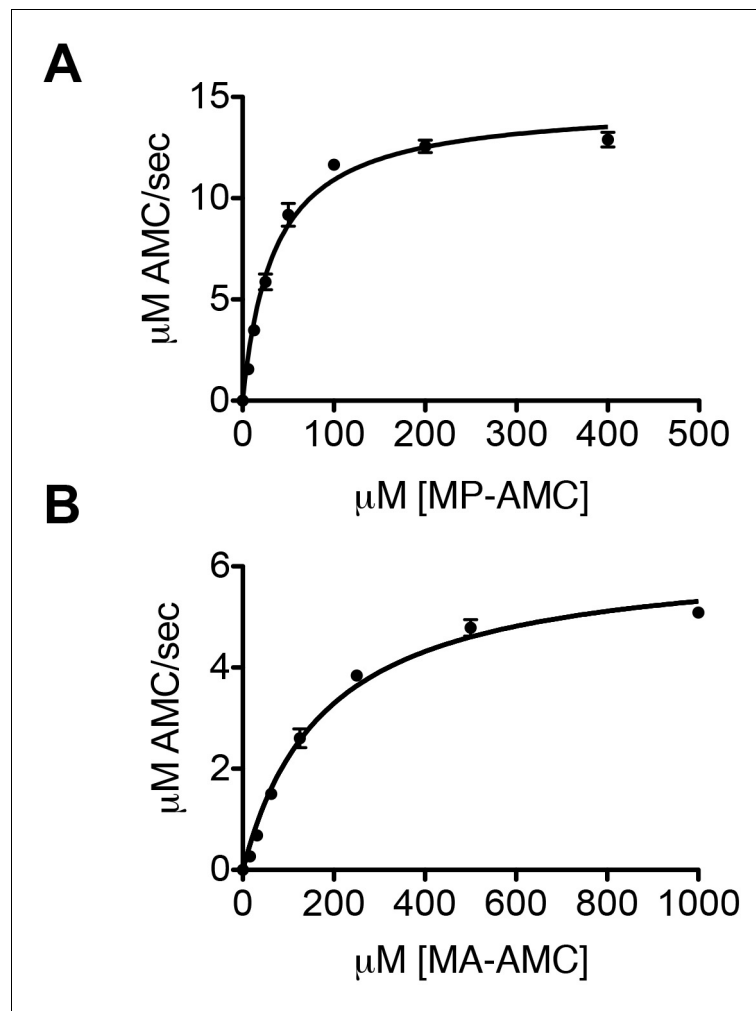
Figure 2—figure supplement 2. DPP9 cleaves after a Xaa-Pro/Ala. (**A**) Hydrolysis of MP-AMC by 12,5 nM recombinant DPP9. An experiment was performed at least three times, each time in triplicates. Shown is a representative Michaelis-Menten analysis, data are represented as mean ± SEM. (**B**) Hydrolysis of MA-AMC by 12,5 nM recombinant DPP9. An experiment was performed at least three times, each time in triplicates. Shown is a representative Michaelis-Menten analysis, data are represented as mean ± SEM.
DOI: 10.7554/eLife.16370.007

A

in vitro cleavage of Syk N-terminal peptide (1-31) by DPP9

MA↓SSGMADSANHLPFFFGNITREEAEDYLVQ

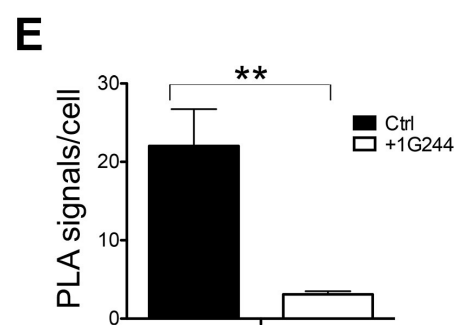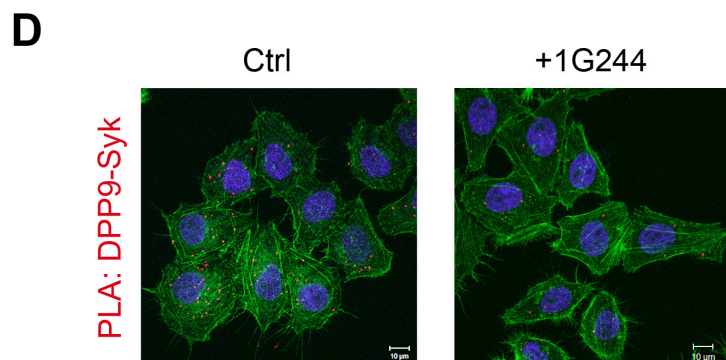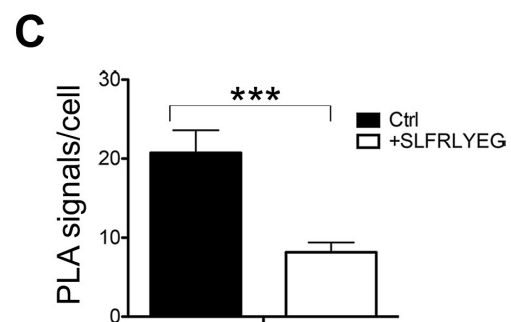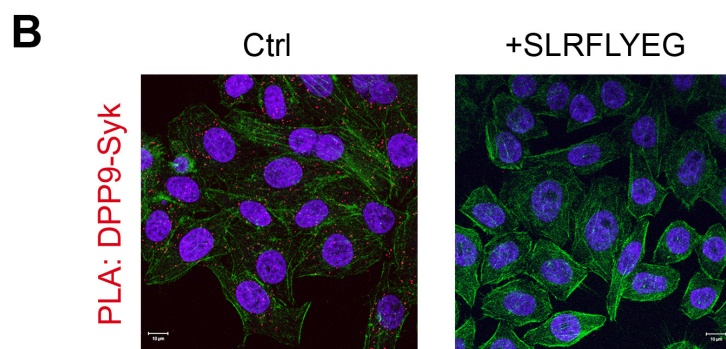| DPP9 wt	DPP9 S730G	inhibitor	% Syk peptide 1-31	% Syk peptide 3-31
-	-	-	99.3	0.7
+	-	-	0.8	99.2
+	-	+	93.8	6.2
-	+	-	99.2	0.8
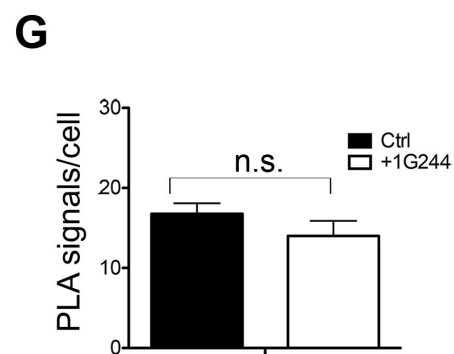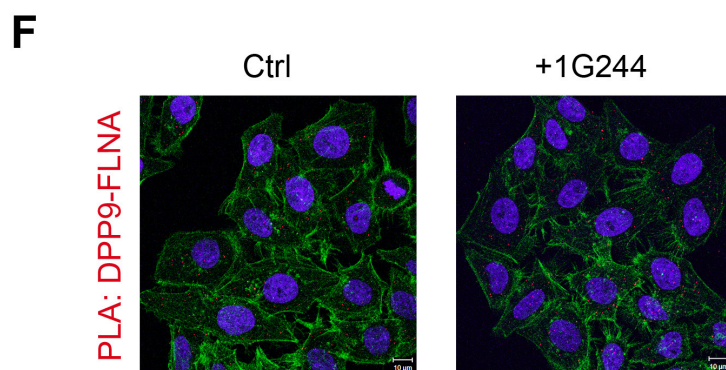
Figure 3. Syk is a novel substrate of DPP9. (**A**) In vitro cleavage of a synthetic Syk peptide corresponding to the N-terminus of Syk (1–31) by recombinant DPP9. 50 µM of a synthetic Syk (1–31) peptide was incubated for 6 hr, either alone or with 130 nM DPP9. For control 10 µM allosteric DPP9

Figure 3 continued on next page

Figure 3 continued

inhibitor SLRFLYEG was added in addition to 130 nM DPP9 and (6 hr). An additional control included the peptide and the inactive DPP9 S730G variant. Samples were analysed by high resolution liquid chromatography/tandem mass spectrometry in triplicate. Quantitation was achieved by extracting ion chromatograms and integrating peak areas for the most abundant 3+ charge state of the intact 1–31 ($[M+3H]^{3+}$ m/z 1149.8589) and the cleaved 3–31 ($[M+3H]^{3+}$ m/z 1082.4997) peptides. The identities and retention times of the peptides were established by accurate mass measurement and product ion spectra (data not shown). (**B–G**) PLA assays showing that the interaction between DPP9 and Syk requires the active site of DPP9. Shown are representative images with the corresponding quantifications of at least three independent PLA experiments. Actin filaments are stained in green, and nuclei were visualized by using HOECHST. The number of PLA signals (red dots) per cell were quantified in a blinded manner using the Duolink ImageTool software (SIGMA). Signals of more than 300 cells were quantified for each condition respectively. Statistical analysis was carried out by an unpaired two-tailed t test (**p<0.005; ***p<0.0005; n.s = not significant). (**B**) The interaction between DPP9 and Syk is markedly decreased in HeLa cells treated with 10 μM SLRFLYEG compared to control cells treated with DMSO. (**C**) Quantification of the PLA DPP9-Syk shown in (**B**). Data are represented as mean ± SEM. (**D**) The number of PLA signals representing DPP9-Syk interactions per cell is reduced upon treatment of HeLa cells with the competitive DPP8/9 inhibitor 1G244 (10 μM, for 5 min) compared to control cells treated with DMSO. (**E**) Quantification of the PLA DPP9-Syk shown in (**D**). Data are represented as mean ± SEM. (**F**) The interaction of DPP9 with FLNA is not significantly altered upon treatment of HeLa cells with 1G244 (10 μM, 30 min) compared to control cells treated with DMSO. (**G**) Quantification of the PLA DPP9- FLNA shown in (**F**). Data are represented as mean ± SEM.
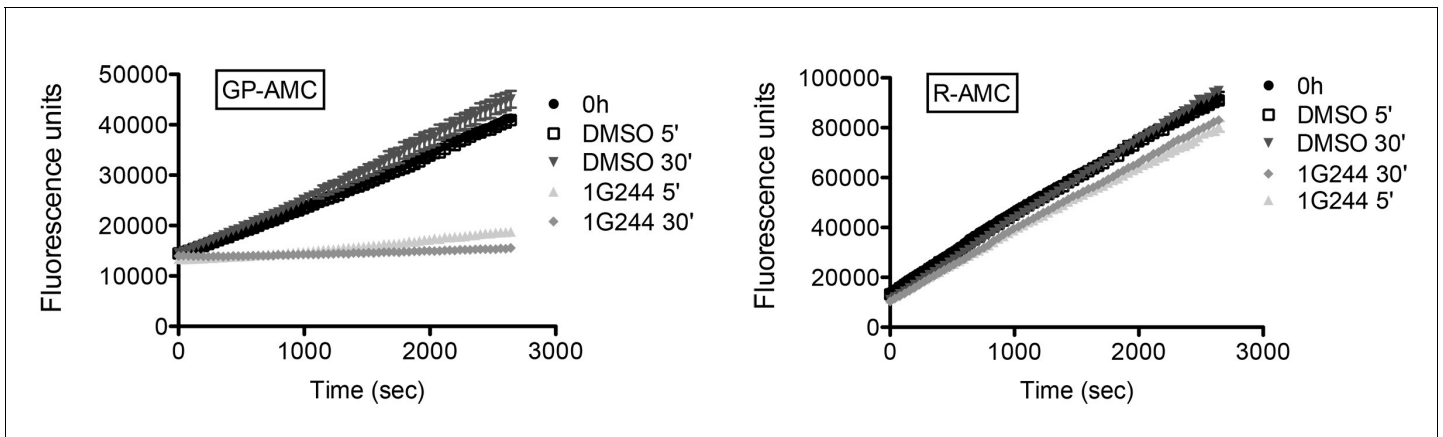
Figure 3—figure supplement 1. Inhibition of DPP activity in HeLa cells with 1G244. HeLa cells were treated with 10 μM DPP8/9 inhibitor 1G244 or DMSO for control (0, 5 and 30 min). Cells were lysed and extracts (5 μg) of were analysed for DPP activity in the presence of the artificial DPP substrate GP-AMC (250 μM) or the unrelated substrate R-AMC (50 μM). Fluorescence was measured over time. Experiment was performed at least three times, each time in triplicates. Shown is a representative, data are represented as mean ± SEM.
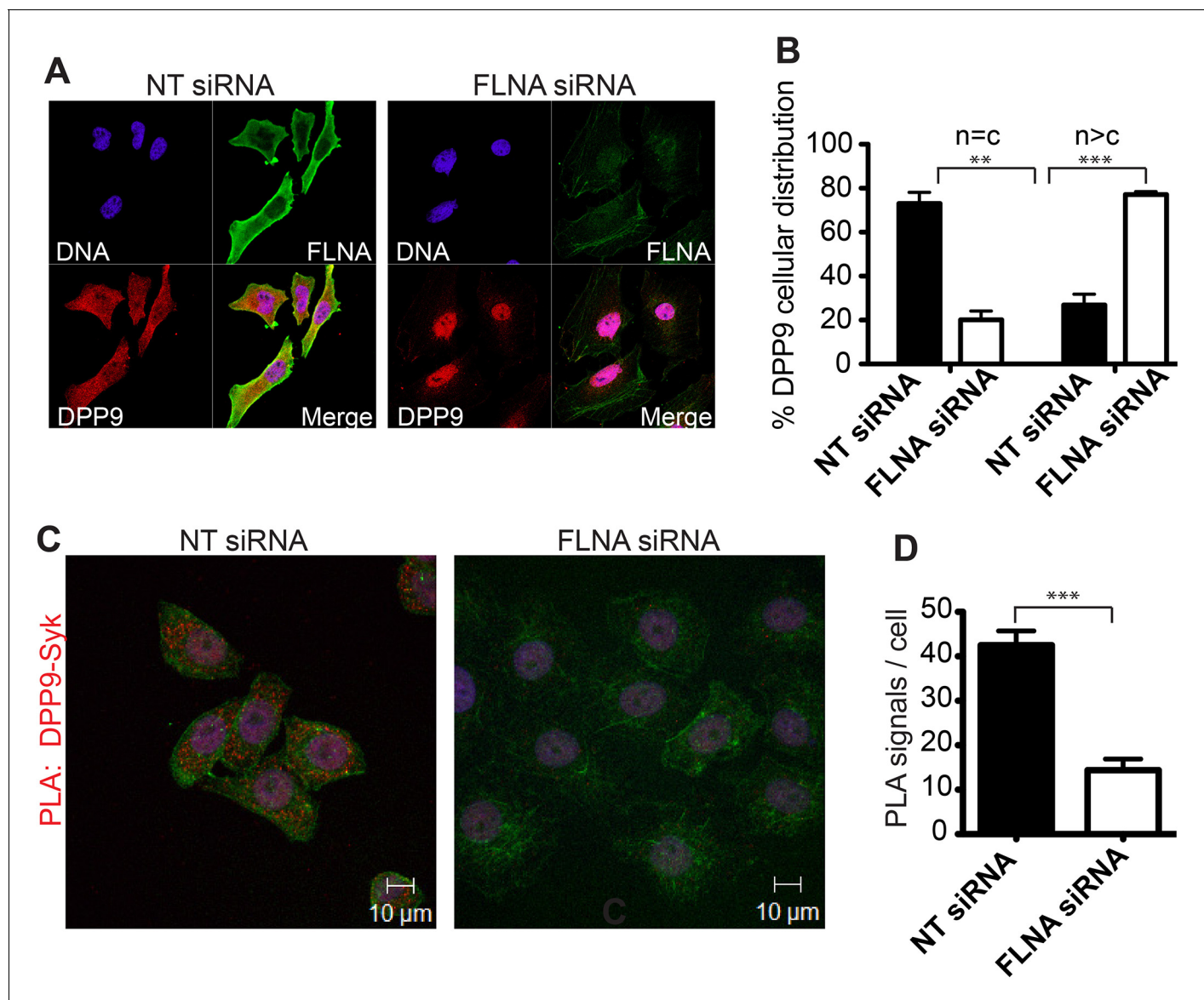DOI: 10.7554/eLife.16370.009

Figure 4. FLNA - a scaffold linking DPP9 to Syk. (**A**) Immunofluorescence images of HeLa cells showing that the cellular localization of DPP9 is altered in FLNA silenced cells. DPP9 is shown in red, FLNA in green and nuclei are visualized with HOECHST staining (blue). Shown are representative images of at least three independent experiments. (**B**) Quantification of the immunofluorescence shown in (**A**). n = c: DPP9 is equally distributed in the cytosol and nucleus; n > c stronger DPP9 staining in the nucleus compared to the cytosol. Data are represented as mean ± SEM. Signals of more than 100 cells for each condition were quantified respectively. Statistical analysis was carried out by an unpaired two-tailed t test (**p<0.005; ***p<0.0005). (**C**) The interaction of DPP9 with Syk depends on the presence of FLNA in HeLa cells. The number of PLA signals (red dots) per cell is markedly decreased in cells treated with FLNA silencing oligonucleotides compared to control cells treated with NT siRNA oligonucleotides. Shown are representative images of at least three independent PLA experiments. (**D**) Quantification of the PLA DPP9-Syk shown in (**C**). Data are represented as mean ± SEM. The number of PLA signals (red dots) per cell were quantified in a blinded manner using the Duolink ImageTool software (SIGMA). Signals of more than 115 cells were quantified for each condition respectively. Actin filaments are stained in green, nuclei were visualized with HOECHST staining. Statistical analysis was carried out by an unpaired two-tailed t test (***p<0.0005).
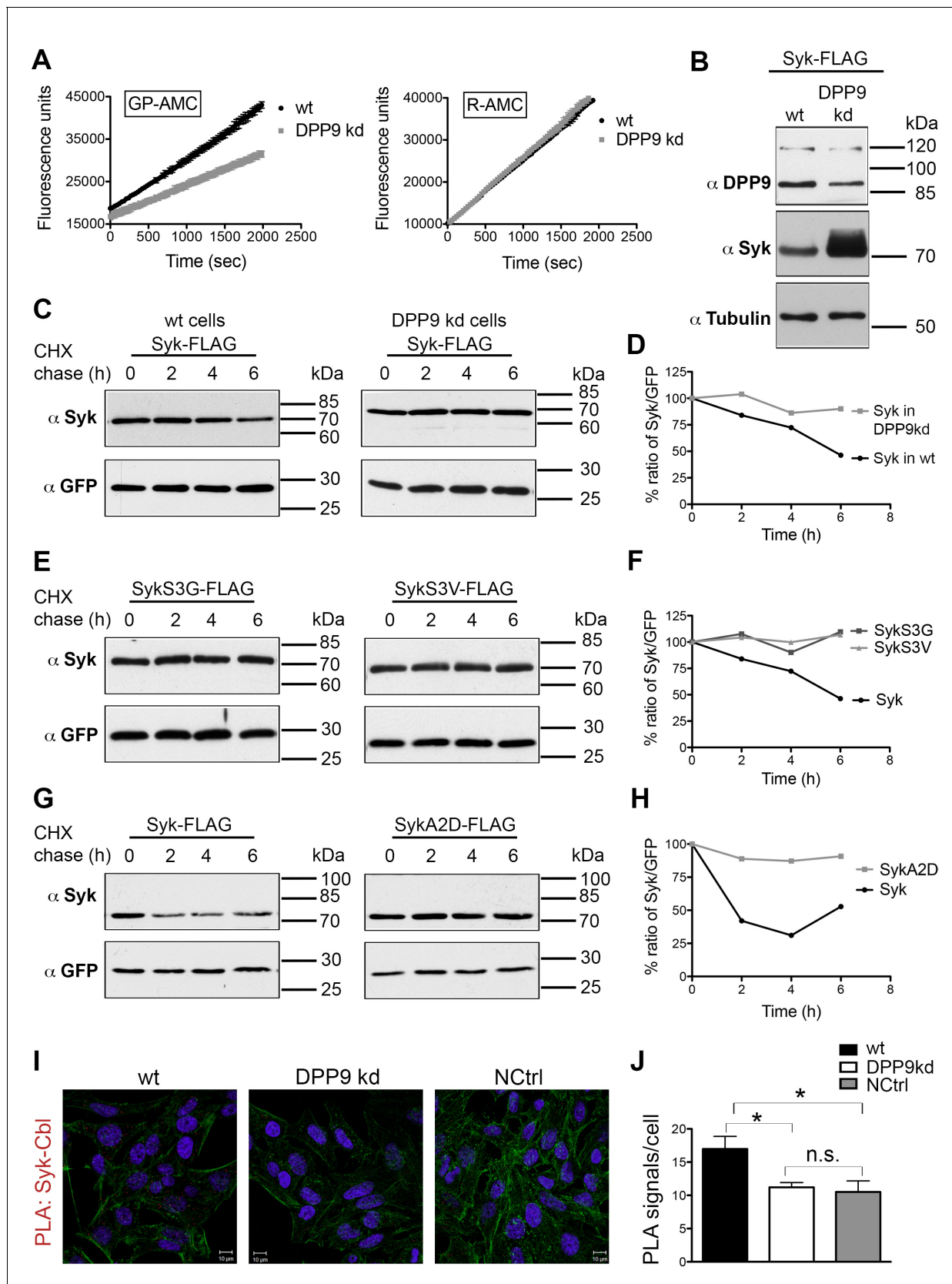
Figure 5. DPP9 determines Syk stability by exposing an N-terminal serine. (**A**) Reduced DPP activity in cytosolic extracts of HeLa cells with a stable silencing of DPP9 (DPP9-kd). Cell extracts either from HeLa wt or DPP9-kd cells (5 μg) were tested for DPP activity using the artificial DPP substrate GP-
Figure 5 continued on next page

Figure 5 continued

AMC (250 µM) or the unrelated substrate R-AMC (50 µM). Fluorescence was measured over time. The experiments were performed at least three times, each time in triplicates. Shown is a representative, data are represented as mean ± SEM. (B) Higher steady-state levels of Syk in DPP9-kd compared to HeLa wt cells. Western blot analysis of cell lysates from HeLa wt or DPP9-kd cells transfected with 1 µg C-terminally FLAG-tagged full-length Syk. Shown is a representative result of at least three independent experiments. Tubulin was analysed as a loading control. (C) Syk stability is determined by DPP9. HeLa wt or DPP9-kd cells were transfected with C-terminally FLAG-tagged full-length Syk and subjected to Cycloheximide (CHX) chase assays. GFP was analysed as a transfection and loading control. Shown is one representative result of at least three independent experiments. (D) Quantification of the Western blot results shown in (C). The ratio of Syk/GFP at time 0 hr was normalized to 100%. For signal quantification GelQuant. NET software provided by biochemlabsolutions.com was used. (E) Syk stability is determined by the serine that is exposed after cleavage by DPP9. HeLa wt cells were transfected with different Syk constructs: Syk-FLAG, SykS3G-FLAG or SykS3V-FLAG and subjected to CHX chase assays. Shown is one representative result of at least three independent experiments. (F) Quantification of the Western blot results shown in (E), as described in (D). (G) Syk stability is increased by mutating the A at position 2 in the DPP9 cleavage site to a D (SykA2D). HeLa wt cells transfected with Syk-FLAG or SykA2D-FLAG were subjected to CHX chase assays. Shown is one representative result of at least three independent experiments. (H) Quantification of the Western blot results shown in (G), as described in (D). (I) Reduced interaction events between Syk and Cbl in the absence of DPP9. Interaction of Syk with Cbl was visualized by PLA in HeLa wt and DPP9-kd cells. The number of PLA signals representing Syk-Cbl interactions per cell was reduced in DPP9-kd cells. For control, cells were treated with only one primary antibody (anti Syk). (J) Quantification of the PLA Syk-Cbl in HeLa cells shown in (I). Data are represented as mean ± SEM. The number of PLA signals per cell were quantified in a blinded manner using the Duolink ImageTool software (SIGMA). Signals of more than 100 cells were quantified for each condition respectively using the Duolink ImageTool (SIGMA). Statistical analysis was carried out by an unpaired two-tailed t test (*$p < 0.05$; n.s = not significant).
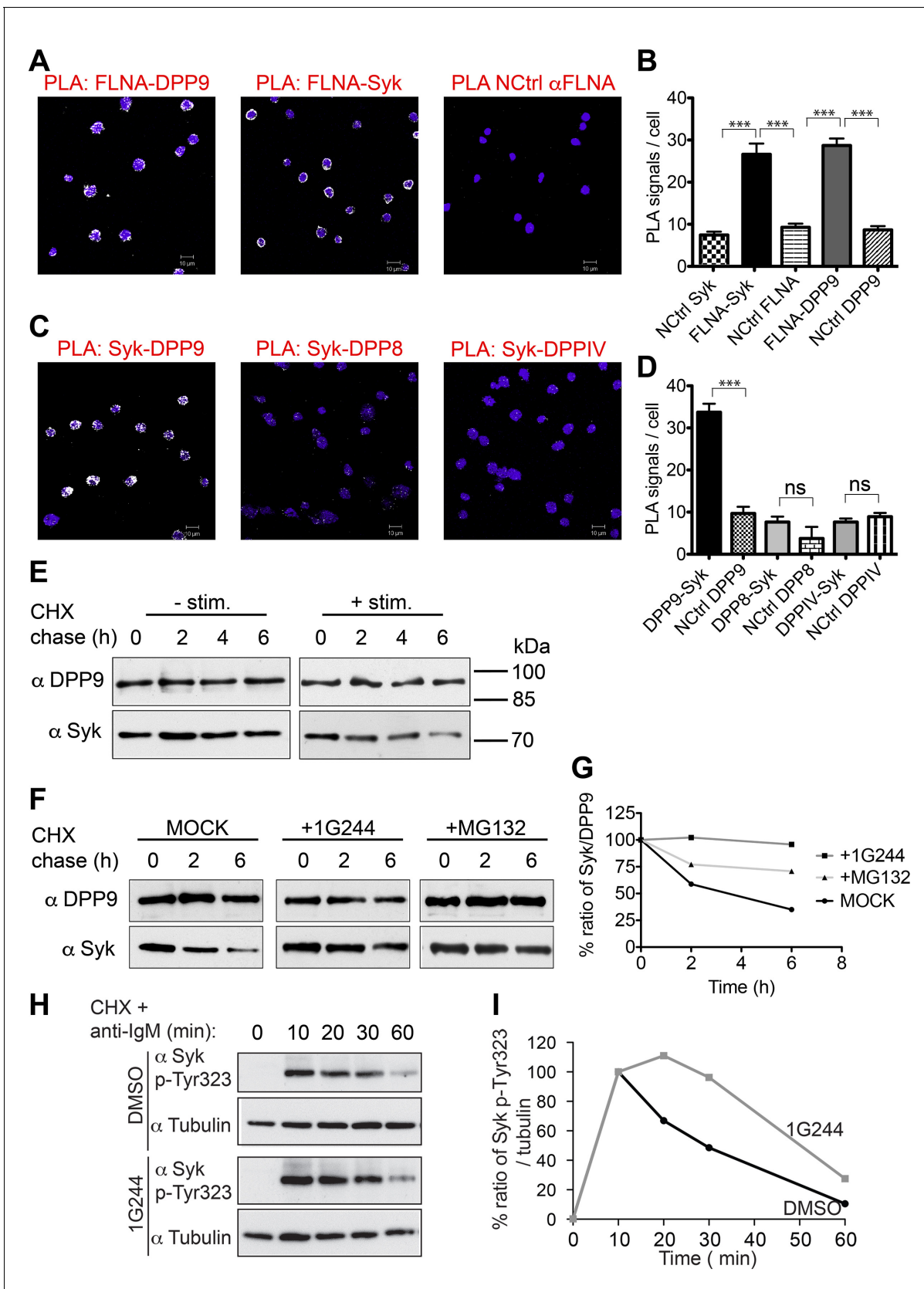
Figure 6. DPP9 regulates the stability of Syk in human Burkitt's lymphoma B cells. (**A** and **B**) PLA showing that the interactions of FLNA with Syk and DPP9 are conserved in human DG-75 B cells. Each PLA interaction is shown here as a white dot, nuclei were visualized by using HOECHST. Control

Figure 6 continued on next page

Figure 6 continued

reactions (NCtrl) were performed with only one primary antibody (αSyk, αFLNA or αDPP9). Shown are representative images and quantifications of at least three independent PLA experiments. The number of PLA signals per cell were quantified in a blinded manner using the Duolink ImageTool software (SIGMA). Signals of more than 80 cells were quantified for each condition respectively. Data are represented as mean ± SEM. Statistical analysis was carried out by an unpaired two-tailed t test (***p<0.0001). (C and D) PLA in DG-75 cells showing that Syk interacts specifically with DPP9 but not with its homologs DPP8 and DPPIV. Control reactions (NCtrl) cells were treated with one primary antibody only: αDPP9, αDPP8 or αDPPIV. Shown are quantifications of the PLA DPP9-Syk, DPP8-Syk and DPPIV-Syk in DG-75 cells from three independent experiments. Data are represented as mean ± SEM. The number of PLA signals per cell were quantified in a blinded manner using the Duolink ImageTool software (SIGMA). Signals of more than 100 cells were quantified for each condition respectively. Statistical analysis was carried out by an unpaired two-tailed t test (***p<0.0001; n.s = not significant). (E) CHX chase experiment showing reduced stability of endogenous Syk upon stimulation of the BCR. Human DG-75 cells were stimulated with 12 μg/ml F(ab')$_2$ fragment goat-anti-human IgG+IgM (+ stim), or left untreated (- stim), and simultaneously subjected to CHX chase. DPP9 was analysed as a loading control. Shown is one representative result of at least three independent experiments. (F) CHX chase experiments showing that the stability of endogenous Syk in stimulated DG-75 cells, is determined by the proteasome and by DPP9. DG-75 cells were treated either with the DPP8/9 inhibitor 1G244 (10 μM), with the proteasome inhibitor MG132 (100 μM) or with DMSO for control (MOCK). Cell lysates were analysed for protein levels of Syk and of DPP9 for loading control by Western blotting. Shown is one representative result of at least three independent experiments. (G) Quantification of the Western blot results shown in (F). The ratio of Syk/DPP9 at time 0 hr was normalized to 100%. For signal quantification GelQuant.NET software provided by biochemlabsolutions.com was used. (H) CHX chase experiment assaying the stability of endogenous phosphorylated Syk (p-Y323) in stimulated DG-75 cells upon treatment with the DPP8/9 inhibitor 1G244 (10 μM) or with DMSO for control (MOCK). Tubulin was assayed as loading control. Shown is one representative result of at least three independent experiments. (I) Quantification of the Western blot results shown in (H). The ratio of Syk p-Y323/tubulin at time 10 min was normalized to 100%. For signal quantification GelQuant.NET software provided by biochemlabsolutions.com was used.
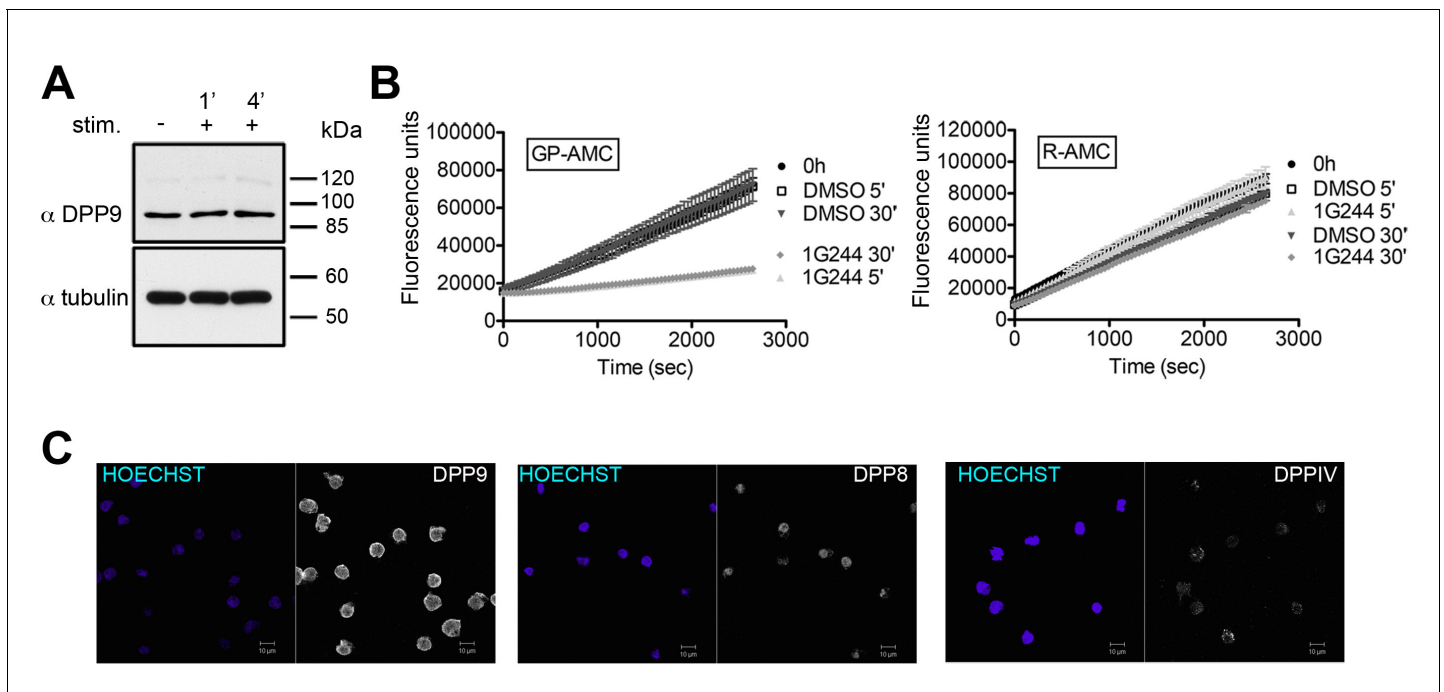
Figure 6—figure supplement 1. DPP9 expression, activity and interaction with Syk in the human DG-75 cells. (**A**) Total cell lysates (10 μg per lane) of DG-75 cells stimulated with 12 μg/ml F(ab')$_2$ fragment goat-anti-human IgG+IgM (0, 1 and 4 min) were analyzed for DPP9 protein levels by Western blotting. Tubulin was used as loading control. Shown is a representative blot, an experiment was performed more than five times. (**B**) DG-75 cells were treated with 10 μM DPP8/9 inhibitor 1G244 or DMSO for control (0, 5 and 30 min). Cell lysates (10 μg) of were analysed for DPP activity in the presence of the artificial DPP substrate GP-AMC (250 μM) or the unrelated substrate R-AMC (50 μM). Fluorescence was measured over time. An experiment was performed at least three times, each time in triplicates. Shown is a representative, data are represented as mean ± SEM. (**C**) Indirect immunofluorescence images of DG-75 cells decorated with antibodies against DPP9, DPP8 and DPPIV.
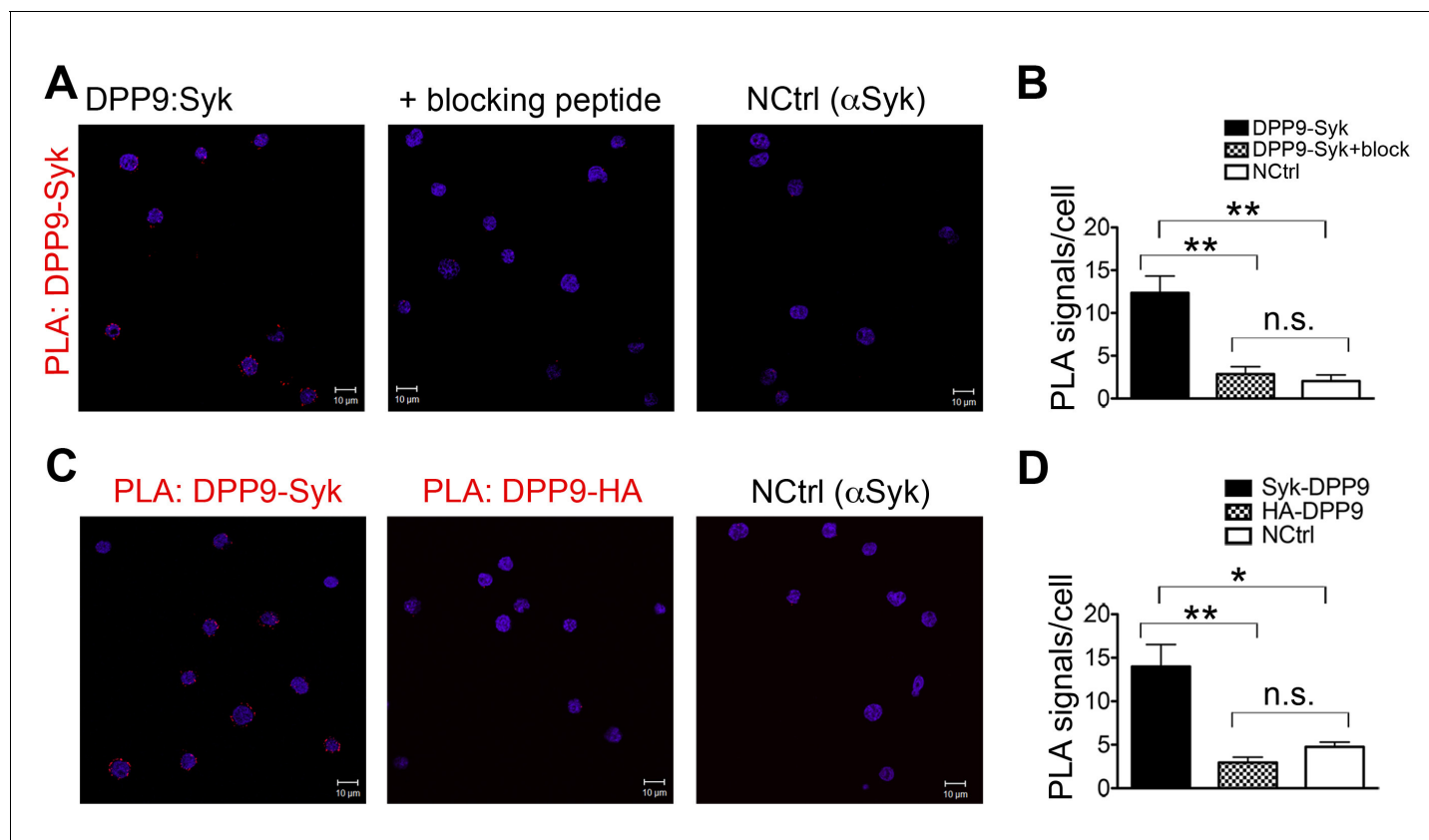DOI: 10.7554/eLife.16370.013

Figure 6—figure supplement 2. Controls for the DPP9-Syk PLA in DG-75 cells. PLA showing the interaction between Syk and DPP9 in DG-75 cells. Nuclei were visualized by using HOECHST. Shown are representative images with the corresponding quantifications of at least three independent PLA experiments. Signals were quantified in a blinded manner using the Duolink ImageTool (SIGMA). (A) Interaction of DPP9 and Syk visualized by PLA in DG-75 cells. The number of PLA signals representing DPP9-Syk interactions per cell was reduced in control samples, in which Syk antibodies were pretreated with a blocking peptide recognized by the Syk antibody. As an additional control, cells were treated with only one primary antibody (here Syk). (B) Quantification of the PLA DPP9-Syk shown in (A). Data are represented as mean ± SEM. Signals of more than 90 cells were quantified for each condition respectively. Statistical analysis was carried out by an unpaired two-tailed t test (**$p < 0.005$; n.s = not significant). (C) Interaction of DPP9 with Syk visualized by PLA in DG-75 cells as in (A). The number of PLA signals per cell was markedly decreased in a control reaction using an unrelated anti-HA antibody instead of the anti-Syk antibody as a second primary antibody for the PLA. As a second control, cells were treated only with Syk antibodies. (D) Quantification of the PLA DPP9-Syk in DG-75 cells shown in (C). Data are represented as mean ± SEM. Signals of more than 77 cells were quantified for each condition respectively. Statistical analysis was carried out by an unpaired two-tailed t test (*$p < 0.05$; **$p < 0.005$; n.s = not significant.
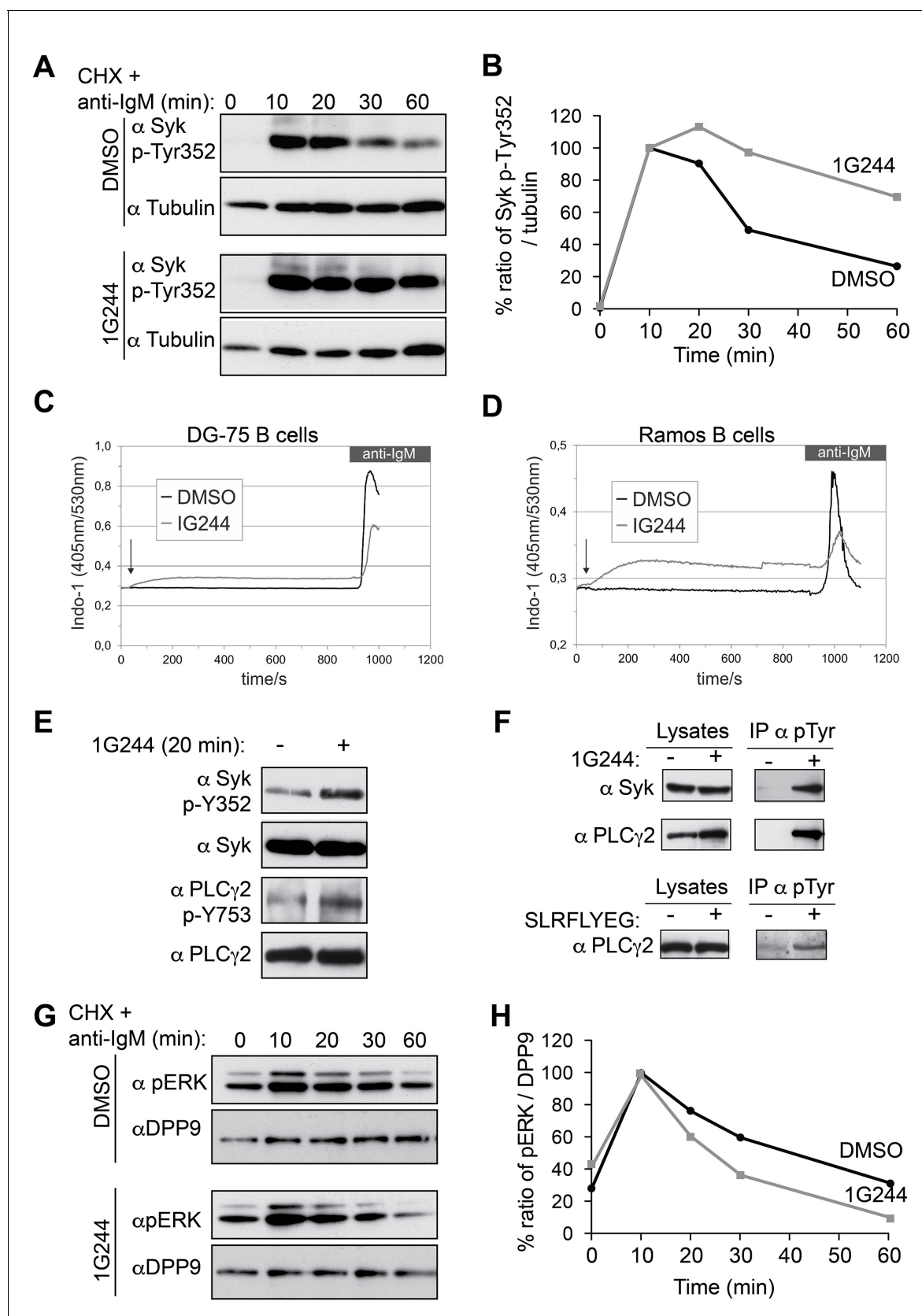
Figure 7. DPP9 targets phosphorylated Syk for degradation thus influencing Syk signalling in B cells, (**A**) Higher levels of endogenous active Syk (phosphorylated on Y352) in stimulated DG-75 cells treated with the DPP8/9 inhibitor 1G244 compared to the mock (DMSO) treated cells. 1G244 (10

Figure 7 continued on next page

Figure 7 continued

μM) was added at the same time of BCR stimulation (time 0). Tubulin was assayed for loading control. Shown is a representative result of at least three independent pulse chase experiments. (**B**) Quantification of the Western blot results shown in (**A**). The ratio of Syk p-Y352/tubulin at time 10 min was normalized to 100%. For signal quantification GelQuant.NET software provided by biochemlabsolutions.com was used. (**C**) Inhibition of DPP9 in DG-75 cells leads to increased Ca^{2+} mobilization, which is not dependant on BCR stimulation. Shown are flow cytometric Ca^{2+} profiles after the addition of 10 μM DPP8/9 inhibitor 1G244 or DMSO for control (marked by an arrow). To monitor Ca^{2+} mobilization upon BCR stimulation in either 1G244-treated or control cells, cells were treated with 10 μg/ml $F(ab)_2$ goat-anti-human IgM. (**D**) Same as in (**C**) using Ramos cells as a second B cell line. (**E–F**) In the absence of BCR stimulation, DPP9 inhibition leads to higher basal levels of phosphorylated Syk and its down stream effector protein PLCγ2. (**E**) Western blotting analysis of DG-75 cells treated with 1G244 in the absence of BCR stimulation. Lysates were analysed with antibodies specific against phosphorylated Syk (p-Y352) or phosphorylated PLCγ2. For loading control lysates were analysed with antibodies recognizing unmodified Syk and PLCγ2. (**F**) Cells were treated for 20 min with 1G244 (10 μM) or DMSO for control. Alternatively, cells were treated for 30 min with the allosteric DPP9 inhibitor SLRFLYEG peptide complexed with the carrier peptide (pep-1). Control cells were treated with the carrier peptide only. Following inhibitor treatment, cells were lysed and subjected to immunoprecipitation assays against Phospho-Y. Eluted proteins were analysed for Syk and PLCγ2 levels by Western blotting. Total protein levels in cell lysates were monitored for control. (**G**) Lower levels of phosphorylated ERK1/2 (both bands) are detected in the 1G244 treated DG-75 cells compared to mock (DMSO) treated cells. 1G244 (10 μM) was added prior to BCR stimulation (time 0). DPP9 was assayed for loading control. Shown is a representative result of at least three independent pulse chase experiments. (**H**) Quantification of the Western blot results shown in (**G**) as described in (**B**).
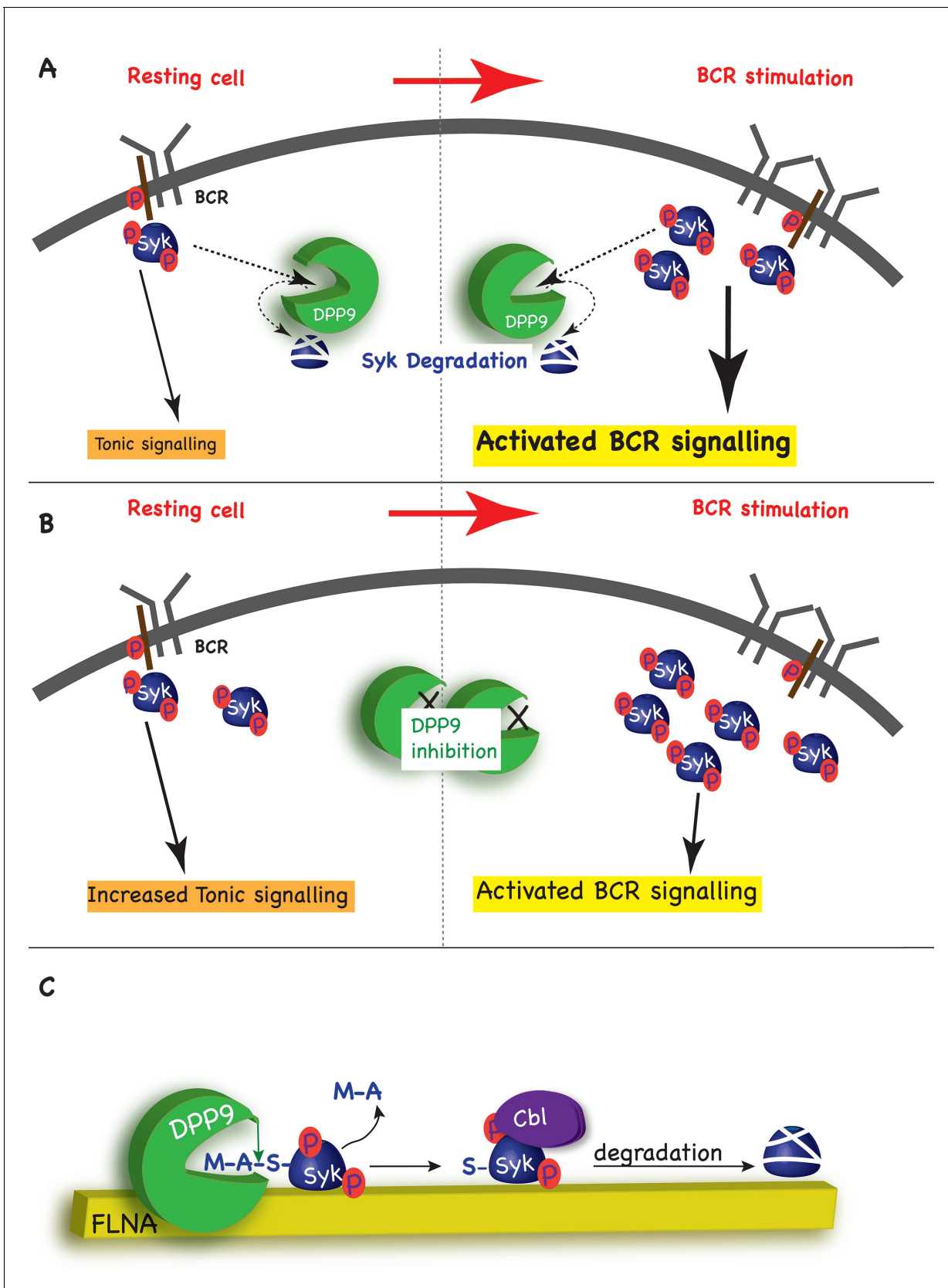
DOI: 10.7554/eLife.16370.015

Figure 8. Model - DPP9 is a negative regulator for Syk signalling, targeting active Syk for degradation by the N-end rule pathway. (**A**) Model: DPP9 regulates Syk signalling. By maintaining low levels of activated Syk in resting B cells DPP9 controls tonic signalling and preserves signalling capacity for

Figure 8 continued on next page

Figure 8 continued

the processes induced by BCR engagement. By targeting Syk for degradation after BCR engagement, DPP9 can also influence the duration of the response to antigen BCR binding. (**B**) Reduced DPP9 activity e.g by inhibition results in higher levels of active Syk in non-stimulated cells. This results in elevated Tonic signalling ('signal leakage'), consequently leading to a lower response upon BCR engagement. (**C**) Model: DPP9 targets Syk for degradation by the N-end rule pathway. In this model, FLNA acts as a recruitment platform for binding of Syk and DPP9. FLNA then supports the cleavage of Syk by DPP9, by increasing the local concentration of Syk and DPP9, stabilizing the interaction between Syk and DPP9, or by optimizing the orientation of DPP9 and Syk. The interaction between DPP and Syk leads to the processing of Syk N-terminus which removes the dipeptide MA, and exposes a neo Syk N-terminus with serine in position 1 is exposed. Subsequently the E3 ligase Cbl binds to Syk p-Y323 initiating its ubiquitintaion and degradation by the proteasome.

DOI: 10.7554/eLife.16370.016